Journal of the Optical Society of Korea, Vol. 2, No. 2, September 1998, pp. 64-73

Effects of Wavelength Dependent Birefringence inside a Fiber Cavity on the Fiber Laser Output Characteristics with a Nonlinear Amplifying Loop Mirror

Ho Young Kim, Kyong Hon Kim, and El Hang Lee

Electronics and Telecommunications Research Institute, Yusong P. O. Box 106 , Taejon 305-606, KOREA

(Received July 8, 1998)

We have theoretically analyzed and experimentally observed the effects of wavelength dependent birefringence inside a laser cavity on the output characteristics of fiber lasers with a figure eight geometry. The spectral and polarization characteristics of fiber lasers are found to be very susceptible to the resultant birefringence composed of the intrinsically existing wavelength dependent birefringence and the externally induced birefringences inside the fiber. For the variation of twist-induced birefringence inside the nonlinear amplifying loop mirror, the laser output power and center wavelength of continuous wave lasers change periodically, but the polarization characteristics remains nearly unchanged. The changes of the birefringence inside the linear loop has little effect on the spectral characteristics but changes the polarization properties such as the polarization direction.

I. INTRODUCTION

Fiber lasers with nonlinear amplifying loop mirrors (NALM) have been developed for potential applications to ultra short light sources [1]- [7]. In the figure eight and linear geometry types, passively mode locked ultra short laser pulses have been generated [1]- [3], and self-started and stable soliton fiber lasers have also been reported [2]. The figure eight geometry is a transformed shape of the fiber ring type cavity, and a linear loop and a NALM are coupled by a direction coupler. In a linear type laser cavity, the rear mirror among two mirrors is replaced by a NALM. In these laser cavities, a NALM has the role of saturable absorber, and modulates the intensity of light proceeding from the NALM to linear parts [7]. The depth of light modulation has been known to depend on the nonlinear phase shift difference between forward and backward propagating light in the NALM, and the total birefringence inside NALM [6,7]. A fiber has the elliptical birefringence which consists of the linear birefringence and circular one. The intrinsic birefringence of normal fiber results from the non-uniformity of the fiber core and is often linear [8,9]. Other birefringences are induced by external perturbations, for examples, bending, twisting or electromagnetic field in the fiber laser cavity. These birefringences have inherent dependencies on the light wave-length and generate the polarization mode dispersion (PMD) between polarization directions [10]. The dependency of the intrinsic linear birefringence is random, and the bending induced birefringence is a linear function of wavelength, but the twist-induced birefringence wavelength has little dependence [9].

In this paper, we discuss the effects of the wavelength dependent birefringence inside the fiber laser cavity with NALM on the laser output characteristics. We model the birefringence of a fiber cavity by the elliptic retarder model [11]. Using the Jones mathematics, the polarization eigenmodes and the transmittance of the laser light from the NALM can be analytically obtained [11], assuming that the two polarization modes experience the same amount of nonlinear phase shifts throughout the cavity [7]. We simulate the effects of intrinsic birefringence and non-linear phase shift with relation to the measured data of polarization mode dispersion (PMD) inside the fiber. In a fiber laser, the characteristics of birefringence, such as the magnitude , the orientation and the ratio between linear and circular birefringence determine the properties of the polarization eigenmodes [11]. Through theoretical analysis, these characteristics are found to have different roles in the transmittance of the NALM. When the orientation of the birefringence inside the NALM varies, the transmittance of the NALM oscillates periodically. The birefringence magnitude determines the oscillating amplitude of transmittance and the ratio of birefringence determines the initial phase of oscillation. We also model the polarization controller (PC) installed in the fiber cavity by the same kind of elliptical retarder. The circular birefringence induced by rotating a PC changes the orientation and ratio of the resultant birefringence. The calculated transmittance

for PC orientation has oscillating behavior similar to that of the ideal quarterwave plate except for its period. We assume that the magnitude, orientation, and ratio of the intrinsic birefringences have random dependence on wavelength. For the rotation of PC in the NALM, the wavelength with maximum transmittance varies randomly. The Er doped fiber laser generates at the wavelength with maximum transmission of the NALM. For the rotation of a PC in the NALM, the output power and center wavelength of the continuous wave are found to oscillate periodically, in good agreement with theoretical predictions. Otherwise, the polarization direction and the polarization state (SOP) of eigenmodes are found to be nearly independent of the birefringence inside the NALM, but to strongly depend on the birefringence of the linear loop.

In section II, we describe the procedure of modeling and the polarization properties of the figure eight type fiber laser and the linear type NALM fiber laser which are predicted by the model. The experimental setup and results are also presented with step by step theoretical analysis. Finally, we conclude the discussion in section III.

II. THE LASER CHARACTERISTICS OF FIBER LASERS WITH NALM

In the theoretical analysis, we assume that nonlinear phenomena in a fiber are very small since the laser operated at low power continuous wave mode.

II. A. THEORETICAL MODELING OF THE FIBER LASER CAVITY

We consider the fiber laser cavities as shown in Fig. 1. These laser cavities commonly have a nonlinear amplifying loop mirror (NALM). A NALM consists of an amplifying fiber and a long normal fiber and a coupler. The amplifying fiber, located asymmetrically in the NALM, is used as the laser medium, and is spliced to one end of the normal fiber. The free ends of the amplifying fiber and the normal fiber are coupled to two ports of a 2×2 ports fiber coupler at one side. The coupling ratio of the coupler is 50/50 and is insensitive to the polarization direction. Two ports of the fiber coupler at the other side are used for a linear loop. In a figure eight laser cavity, two ports in the linear loop are connected together, including an isolator and another fiber coupler for laser output. In a linear type laser cavity, called an alpha laser cavity, only one port is used and connected to an output mirror. At one end of this normal fiber toward the coupler in the NALM, a polarization controller, PC1, is installed. In the linear loop, the same type of a polarization controller, PC2, is also installed after the isolator and toward the

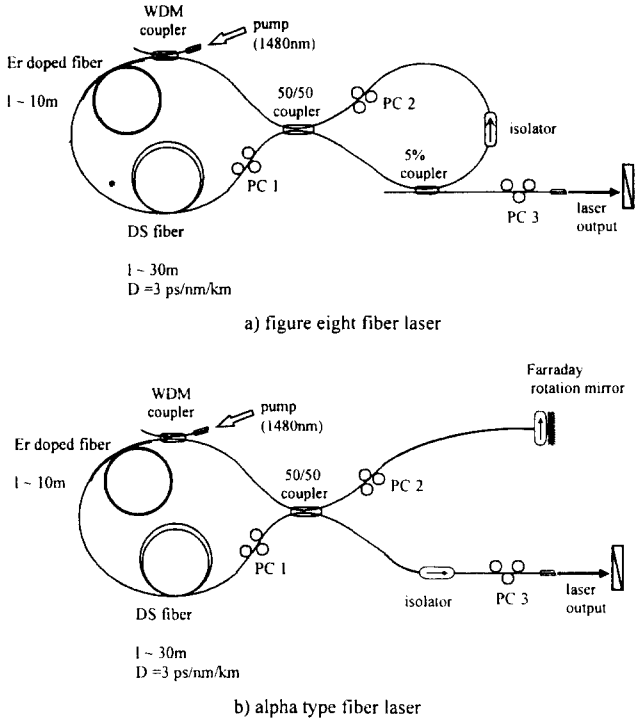

FIG. 1. Schematic diagrams of fiber lasers with a nonlinear amplifying loop mirror, (a) figure eight type, (b) linear type.

NALM, as shown in Fig. 1.

Here, we start to follow the light from the position, "1", at the ouput port of the output coupler in the linear loop, and look into the evolution of polarization step by step. We use the light traveling coordinate system. Incident laser light from the linear loop to the input port of the NALM is divided into two directions, one in the clockwise direction and the other in the counter-clockwise direction with equal amplitudes and a $\pi/2$ phase difference with respect to each other. The two light waves propagate in the opposite directions through the NALM, and experience different birefringences, denoted by O^{cw} and O^{ccw}, respectively. Additionally, the y-axis of the clockwise traveling light is inverted at the coupler two times before and after light travels through the NALM. Without the non-reciprocal elements in the NALM, the birefringence is reciprocal, and $O^{ccw} = P(O^{cw})^T P$, where P has a function of y axis inversion at ports of the coupler and is expressed as $P = \begin{bmatrix} 1 & 0 \\ 0 & -1 \end{bmatrix}$ [12].

They also experience different nonlinear phase shifts proportional to their intensities. These phase shift are assumed to be given as $\phi_{NL}^{cw} = n_2 I^{cw} l$ and $\phi_{NL}^{ccw} = n_2 I^{ccw} l$, respectively [7], where $n_2 = 3.2 \times 10^{-16} cm^2/W$, and I^{cw} is the intensity of clockwise traveling light and I^{ccw} is the intensity of counter-clockwise (CCW) traveling light. Though the intensities of the two light waves at the ports of the cou-

pler are almost the same, the intensity of the traveling waves in the NALM vary with the position of the fiber cavity. CCW traveling light is first amplified through the Er doped fiber laser and experiences a nonlinear phase shift through the normal fiber much larger than the nonlinear phase shift that the colockwise light experiences before being amplified. When they are combined at the end of the coupler, the difference of nonlinear phase-shift between two lights, $\Delta\phi_{NL} = (\phi_{NL}^{ccw} - \phi_{NL}^{cw})/2$. Thus, the net birefringence, O, for the incident laser light through the NALM, is obtained as $O = [e^{i\Delta\phi_{NL}}O^{cw} - e^{-i\Delta\phi_{NL}}P(O^{cw})^T P]/2$. The birefringence in a fiber with length l is generally elliptical, and consists of linear birefringence β and circular birefringence, α. Three parameters, such as the magnitude $\delta(= \sqrt{\alpha^2 + \beta^2}\, l)$, the azimuth angle A to the fast axis of the fiber, and the ellipticity parameter $B(= [\tan^{-1}(\alpha/\beta)]/2)$, describe thoroughly the characteristics of the birefringence [8].

Using the Jones matrix for the birefringence model [11], the net birefringence, O, can be expressed as

$$O = \begin{bmatrix} i(a+bi)\sin\Delta\phi_{NL} & i\cos\Delta\phi_{NL} + id\sin\Delta\phi_{NL} \\ ic\cos\Delta\phi_{NL} - id\sin\Delta\phi_{NL} & i(a-bi)\sin\Delta\phi_{NL} \end{bmatrix} \quad (1)$$

where $a = \cos\delta/2$, $b = \cos 2B\cos 2A\sin\delta/2$, $c = \cos 2B\sin 2A\sin\delta/2$, and $d = \sin 2B\sin\delta/2$. The laser output must satisfy the resonance condition in such a way that the optical wave has to come back to the same phase and SOP after one round trip inside the laser cavity [13]. The eigenvectors of the corresponding Jones matrix, O, satisfy the requirements obtained from the following eigenvalue equation,

$$Ou_{\pm} = \lambda_{\pm}u_{\pm} = \sqrt{T_{\pm}}\exp(\pm i\eta_{\pm})u_{\pm} \quad (2)$$

where $\lambda_{\pm}$ are the eigenvalues for the eigenvectors and $T_{\pm}$ are the squares of the absolute value (called as the transmittances of the NALM) and $\eta_{\pm}$ are the phases of the eigenvalues. These eigenvectors satisfy the resonance condition for the polarization. These eigenvectors are the polarization eigenmodes for the total birefringence experienced during one round trip. Eq.(2) explains that the eigenmodes have a phase difference during one round trip. The frequency difference between the eigenmodes, or the PMB frequency, f_p, is obtained by dividing this phase difference by one round trip time through laser cavity , expressed as,

$$f_p = \frac{|\eta_+ - \eta_-|c}{2\pi nl}. \quad (3)$$

Here, we temporarily drop the term for birefringence and nonlinear phase shift of the linear loop for simplification. Then, the evolution of the polarization state of laser light through this figure eight fiber cavity can be analyzed by the above simple matrix, O. The eigenvalues of these polarization eigenmodes through the NALM, $\lambda_{\pm}$, can be expressed as follows :

$$\begin{aligned}\lambda_{\pm} &= ia\sin\Delta\phi_{NL} \pm \sqrt{(b^2+d^2)\sin^2\Delta\phi_{NL} - c^2\cos^2\Delta\phi_{NL}} \\ &= i\cos(\delta/2)\sin\Delta\phi_{NL} \pm \sqrt{((\cos^2 2B\cos^2 2A + \sin^2 2B)\sin^2\Delta\phi_{NL} - \cos^2 2B\sin^2 2A\cos^2\Delta\phi_{NL})\sin^2(\delta/2)}. \quad (4)\end{aligned}$$

II. B. TRANSMITTANCE OF NONLINEAR AMPLIFYING LOOP MIRROR

At first, we consider the simple system which has a quarter-wave plate in the NALM and no birefringence in other components. Calculating the Jones matrix of the quarter-wave plate with the parameters $B = 0.0$ and $\delta = \pi/2$ from Eq. (4), the transmittance of the NALM can be obtained as,

$$T_{\pm} = \left|i\sin\Delta\phi_{NL} \pm \sqrt{\cos^2 2A\sin^2\Delta\phi_{NL} - \sin^2 2A\cos^2\Delta\phi_{NL}}\right|^2/2. \quad (5)$$

When $\Delta\phi_{NL} = 0.0°$, $T_{\pm} = (\sin 2A)^2/2$, i.e. the transmittance of the NALM has a sinusoidal function for the orientation of the quarter-wave plate to the fiber axis, as shown in curve (1) of Fig. 2. When the pump power is large and $\Delta\phi_{NL} = 180°$, $T_{\pm} = 1-(\sin 2A)^2/2$, and displays the function of the quarter-plate orientation, A, inverse to a curve (1). A polarization controller has been known to play a role as a quarter-wave plate [14]. However, the polarization controller is not exactly the same as the quarter-wave plate. Fig. 3 shows the schematic structure of the polarization controller. It consists of three parts with respect to the externally induced birefringence inside the fiber. Part No. 1 (see in Fig.3) has bending induced birefringence with 90°

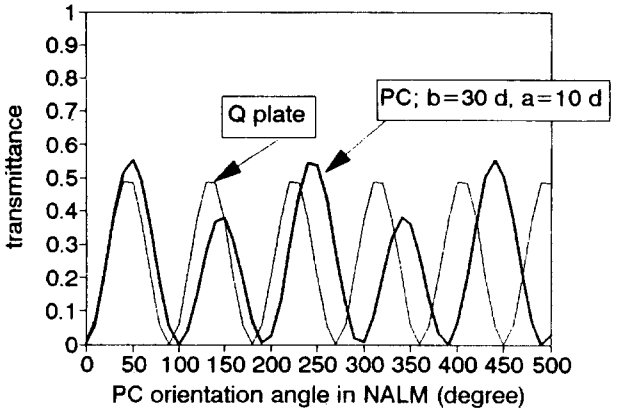

FIG. 2. Calculated transmittances of the NALM for the variations of the quarter wave plate orientation angle (curve (1)) and the PC orientation angle (curve (2))in the NALM, assuming that linear birefringence inside the NALM is 30°/m.

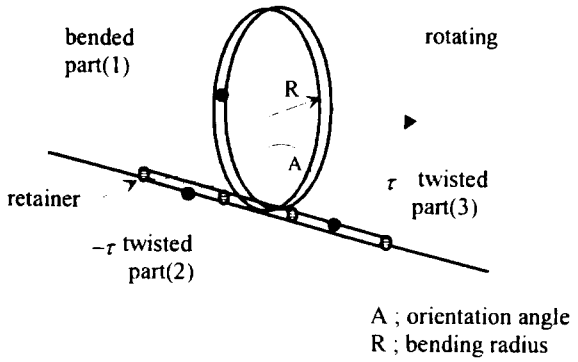

FIG. 3. Schematic of a polarization controller.

magnitude, added to the intrinsic birefringence. Parts No. 2 and No. 3 have twist induced birefringence, but the directions of twist inside fibers are opposite to each other. Then, the Jones matrix for the birefringence inside PC can be obtained by the products of three different matrices. After some calculations, the transmittance of the NALM can be obtained as,

$$T_{\pm} = \left| i \sin \Delta\phi_{NL} + \sqrt{\cos^2(2-g)\theta \sin^2 \Delta\phi_{NL} - \sin^2(2-g)\theta \cos^2 \Delta\phi_{NL}} \right|^2 /2. \quad (6)$$

where θ is the orientation angle of the PC and g is about 0.15 [8], assuming that the intrinsic birefringence inside the fiber of PC is negligible. Since Eq.(6) differs from Eq.(5) only by the replacement of $(2-g)\theta$ by "2A", the rotation angle of PC corresponds to about 0.92 of a quarter plate rotation angle [8], as shown in a curve (2) of Fig. 2.

Now, we introduce wavelength dependent birefringence inside the fibers of the NALM. In our experiments, a dispersion shifted fiber (DSF) with 2 ps/nm/km dispersion at 1550 nm was used as the previously mentioned normal fiber and had the wavelength dependent birefringence measured with a polarization analyzer, as shown in the solid curve of Fig. 4. This birefringence might be mainly induced from the core ellipticity, since other birefringences cannot have similar wavelength dependence in the wavelength region from 1400 nm to 1600 nm [9]. Twist induced birefringence has little wavelength dependence, and stress birefringence has dependence inversely proportional to the wave-length [9]. Here, we investigate the effects of intrinsic birefringence parameter by parameter, δ, "A", and "B". Figure 5 shows the transmittances of the NALM as a function of the magnitude of the linear birefringence inside the DSF, δ, when the birefringence

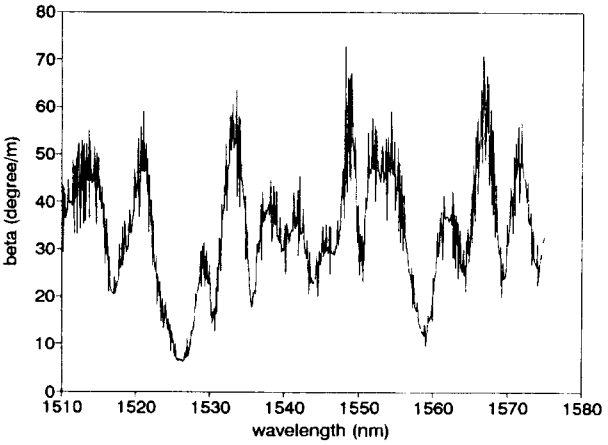

FIG. 4. Wavelength dependence of the intrinsic birefringence inside the dispersion shifted fiber.

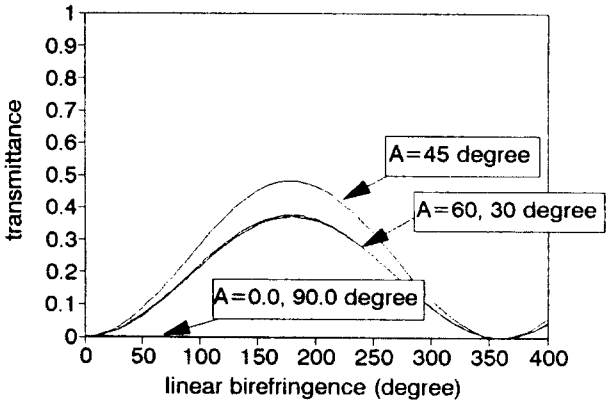

FIG. 5. Calculated transmittance of the NALM as a function of birefringence magnitude inside the DSF.

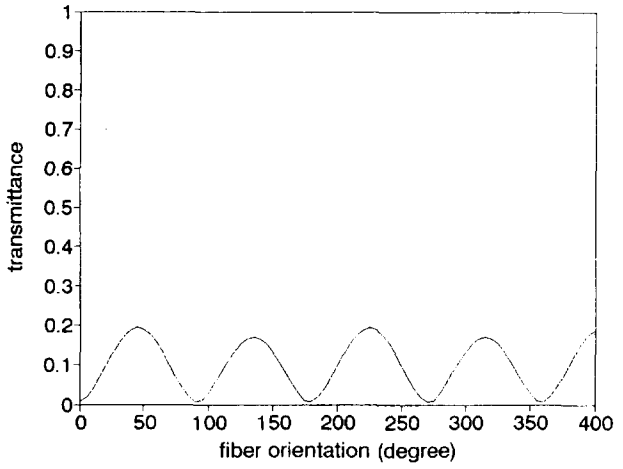

FIG. 6. . Calculated transmittance of the NALM as a function of birefringence orientation angle in the NALM, assuming that linear birefringence inside the NALM is 30°/m.

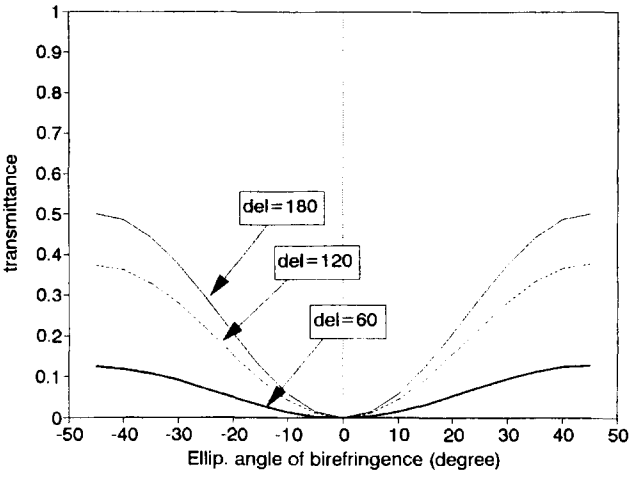

FIG. 7. Dependence of transmittance on the ellipticity of birefringence.

is assumed to be linear and there is no nonlinear phase shift. When the birefringence is aligned with the fast axis, the transmittance vanishes. The transmittance oscillates with 180° periodicity. As the birefringence orientation varies, the transmittance reveals an oscillation with 90° periodicity as shown in Fig.6. When the birefringence inside the DSF becomes circular, the transmittance is found to increase, as shown in Fig.7.

Including PC, the Jones matrix for the net birefringence can be obtained by products of the PC matrices and the matrix for the fiber. After straightforward calculations, the transmittance can be modified from Eq.(6) as following;

$$T_{\pm} = \left| ia_m \sin\Delta\phi_{NL} \pm \sqrt{(b_m^2 + d_m^2)^2 \sin^2\Delta\phi_{NL} - c_m^2 \cos^2\Delta\phi_{NL}} \right|^2 \tag{7}$$

where $a_m = a - b\cos(2-g)\theta - c\sin(2-g_\theta$, $b_m = b + a\cos(2-g)\theta + d\sin(2-g)\theta$, $c_m = c - d\cos(2-g)\theta + a\sin(2-g)\theta$, $d_m = d + c\cos(2-g)\theta - b\sin(2-g)\theta$, and θ is the orientation angle of the PC. As the PC1 orientation angle varies, the transmittances vary sinusoidally with equal periods and the same starting points, but the maximum amplitudes vary, depending on the linear birefringence magnitudes, as shown in Fig. 8. As previously mentioned, the transmittance has little dependence on the PC orientation at multiples of 180°. Possibly a small amount of offset of the birefringence to the fast axis, such as 10 degree, produces the alternatively strong and weak oscillation of the transmittance, as shown in a curve (2) of Fig. 2. The NALM with other values of the ellipticity angle, B, has much different orientation angles and magnitude of maximum with respect to each other as shown in Fig. 9. These theoretical predictions agree well with the experimental results as shown in Fig. 10 and Fig. 11. For experimental study, an Er doped fiber laser of figure eight configuration was constructed as shown in Fig. 1. A 10 m long Er fiber with doping rate 450 ppm and a 23 m long dispersion shifted fiber (DSF) with 3.5 ps/nm·km dispersion at 1550 nm were used for the laser cavity with 50 m total length. A 1480 nm pumping laser was used with a wavelength multiplexing coupler. Laser output was taken from one port of the fiber coupler with 5 % coupling ratio in the linear loop. At 1545 nm, the linear birefringence was 660° (corresponding to 29° /m). At 1570 nm, the transmit-

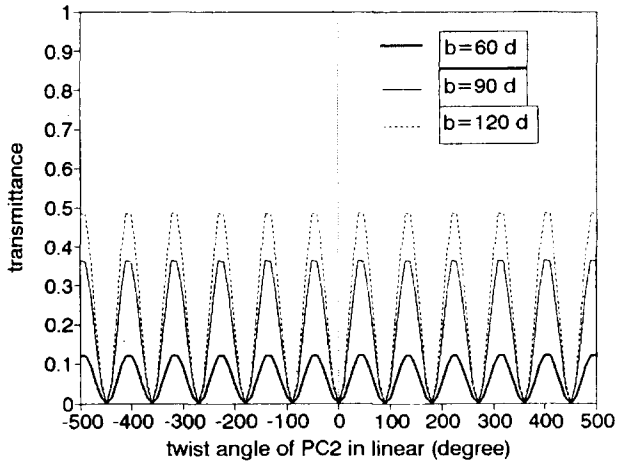

FIG. 8. Calculated transmittance of the NALM as a function of PC orientation angle in the NALM with birefringence of 30.0°/m (heavy solid line curve), 45.0° (solid line curve), and 90.0° (dashed line curve).

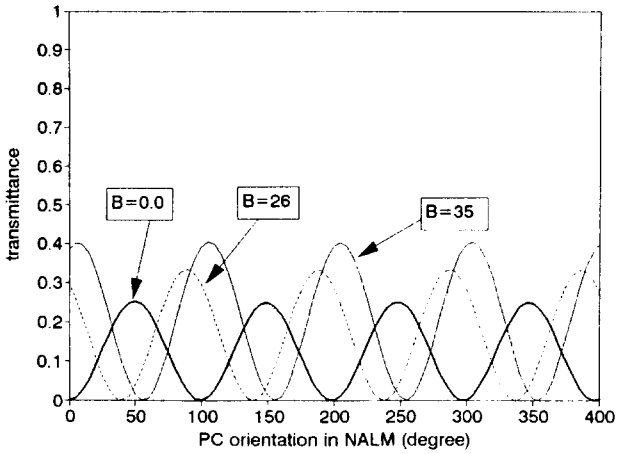

FIG. 9. Calculated transmittance of the NALM as a function of PC orientation angle in the NALM with birefringence of 0.0° ellipticity (heavy solid line curve), 26.0° (solid line curve), and 30.0° (dashed line curve).

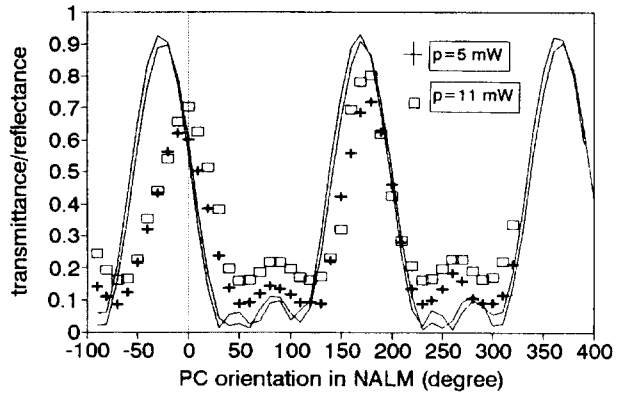

FIG. 10. Measured (crosses and boxes) and theoretical (solid line curve) data for the transmittance of the NALM as a function of PC orientation angle, at 1545 nm of CW laser.

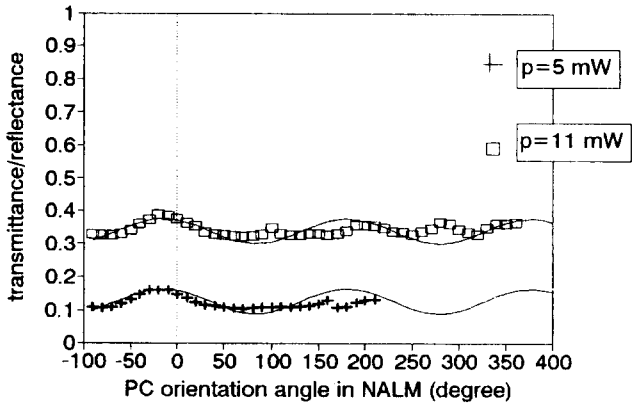

FIG. 11. Measured (crosses and boxes) and theoretical (solid line curve) data for the transmittance of the NALM as a function of PC orientation angle, at 1570 nm of CW laser.

tance showed weak dependence on the PC orientation in good agreement with theoretical predictions for the NALM with 894.7° (38.9° /m) linear birefringence, as shown in Fig.11. In both cases, the nonlinear phase shifts, $\Delta\phi_{NL}$, and the orientation, "A", are set to 20° and 30°, respectively.

Athough the intrinsic birefringence inside the DSF is not large, the accumulation of phase retardation through the 23 m long DSF has a very strong effect on the transmittance of the NALM with respect to the wavelength of the light-wave.

II. C. SPECTRAL CHARACTERISTICS OF FIBER LASERS WITH WAVELEGNTH DEPENDENT BIREFRINGENCES

Here, we investigated the wavelength dependence of the laser output characteristics with the NALM. At first, we discussed the CW laser output at a fixed wavelength. A polarization insensitive wavelength tunable filter with 1 nm optical bandwidth was installed inside the linear loop of the figure eight fiber laser cavity. From this experimental setup, we obtained experimental results for the CW lasing at 1545 nm and 1564 nm, as shown in a curve (1) and curve (2) of Fig. 12. With the filter, laser light can be generated only at a fixed wavelength. The laser output power at a fixed wavelength depends only on the transmittance of the NALM which is a function of PC orientation, as previously discussed. Therefore, the laser output power changes in close relation to the orientation of the PC. When the transmittance is very low, the total gain inside the fiber cavity is below the threshold for lasing and the laser generation ceases, for example, at PC orientations ranged from 40° to 130° with 1545 nm lasing (see a curve (1) of Fig. 12). The experimental results agreed qualitatively with the theoretical predic-

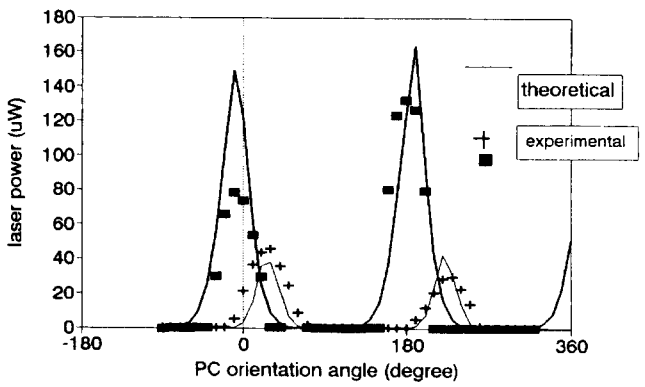

FIG. 12. Laser powers as a function of PC orientation angle at 1545 nm (experimental; squares (1), theoretical; solid line curve (3)) and 1560nm (experimental; crosses (2), theoretical; solid line curve (4)) with 11 mW pump power.

tions (as shown in a curve (3) and (4) of Fig.12) using the gain model and numerical iterations for the CW laser rate equations.

Next, we discussed the case of multi wavelength operation inside a fiber laser cavity. Considering that the laser gain medium is homogeneous and strong competition exists between modes in gain, we model the laser dynamics such that the laser generates at the wavelength with the greatest magnitude of the total gain, $G = g_a T_{NALM} \Delta T_{NALM}$, in the optical band, where g_a is the gain in the Er fiber and T_{NALM} is the transmittance of the NALM and ΔT_{NALM} is the slope of the transmittance with the variation of the nonlinear phase shift at a wavelength. When three wavelengths are concerned, the total gains of the NALM at each wavelength oscillate as shown in a curve (1), curve (2), and curve (3) of Fig.13 for the variation of PC inside the NALM, assuming that gains in the laser medium are the same. Owing to the choice of the greatest one, the wavelength of the laser changes as shown in Fig.14. By this simple modeling, we will explain the reason

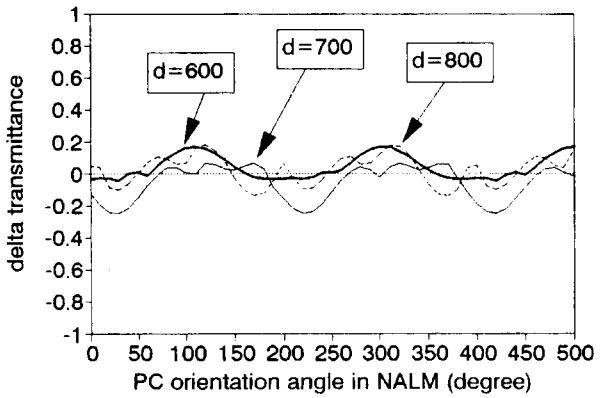

FIG. 13. Transmittance derivatives, ΔT_{NALM}, of the NALM for the variation of PC orientation angle in the NALM with the birefringence of 600.0° ellipticity (heavy solid line curve), 700.0° (solid line curve), and 800.0° (dashed line curve).

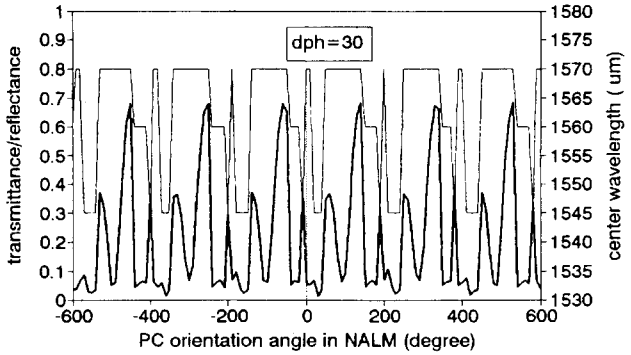

FIG. 14. Transmittance (heavily solid curve) and center wavelength (solid line curve) as a function of PC orientation angle (theoretical results).

that the center wavelength of the CW laser in the fiber lasers with the NALM changed with periodic patterns.

Instead of the measured data for the laser medium gain and the birefringence inside the DSF depending on the wavelength of the light wave, we assumed the values in Fig. 15. With these models, the transmittances and center wavelengths of the CW laser for the variation of the PC orientation in NALM at 11 mW pump power are calculated as shown in solid line curves of Fig. 16 and Fig. 17, respectively. The measured results of laser output powers and center wavelength at 12 mW pump power were star dotted datas in Fig. 16 and Fig. 17, respectively. Experimental results showed the periodic behaviors. The center wavelength changed with special patterns when the PC orienation changed, in a qualitative agreement with theoretical predictions, having some discrepancies. Mostly, CW laser generates at 1560 nm with the highest medium gain, and

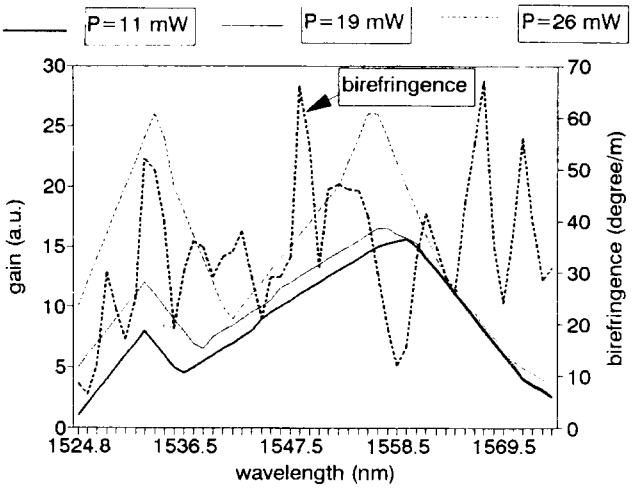

FIG. 15. Gain (heavily solid curve) of the amplifying fiber and birefringence (solid line curve as a function of a laser wavelength.

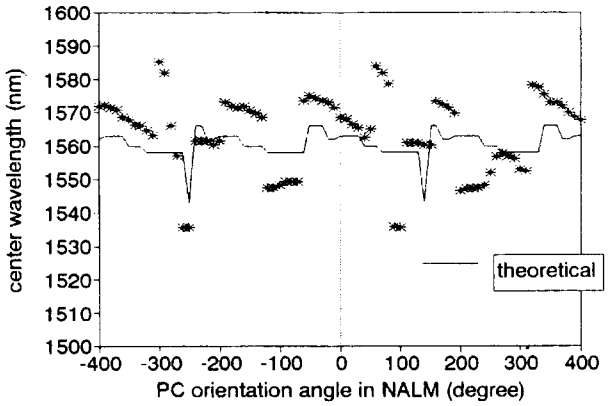

FIG. 16. Center wavelengths as a function of PC orientation angle at 11 mW pump power (stars; experimental results, solid line curve; theoretical results).

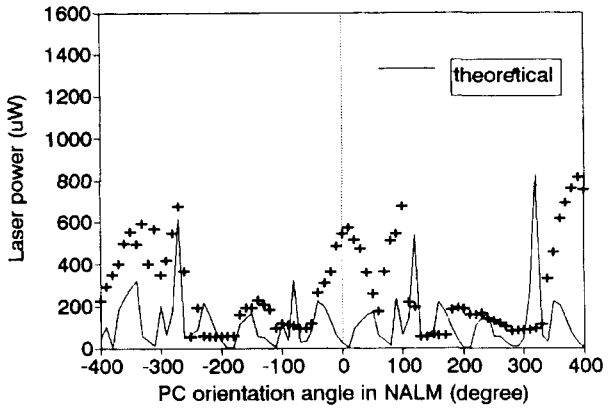

FIG. 17. Laser power (crosses) and transmittance (solid line curve) as a function of PC orientation angle at 11 mW pump power.

suddenly jumped to 1530 nm or 1570 nm when highest mode for total gain inside the fiber cavity was altered by the change of the birefringence. As the laser power does not directly correspond to the transmittance, measured data revealed many differences from theoretical predictions. However, they showed the dependence of laser powers on the intrinsic birefringence. Further analysis based on the high order nonlinear phenomena will make them clear in the near future.

II. D. POLARIZATION CHARACTERISTICS OF FIBER LASERS WITH NONLINEAR AMPLIFYING LOOP MIRROR

Linear loop has a normal fiber with ~2 m length, a polarization controller, PC2, and an isolator for preventing the laser light from propagating in the opposite direction. The laser light travels in only one direction through the linear loop and experiences a different birefringence and nonlinear phase shift. Since the light does not experience the evolution of polarization through the output coupler and the isolator, the evolution of polarization of traveling light waves depends only on the birefringence inside the DSF of the linear loop. The birefringence inside the DSF of the linear loop, denoted by O^l, has magnitude δ_1, azimuth A_1, and ellipticity parameter B_1. The Jones matrix, O^T, for a net birefringence of the figure eight fiber cavity is multiplexed by that of a linear loop, O^L, and can be expressed as $O^T = O^L O$.

After the same procedures as in the previous section, the transmittance through the fiber laser cavity, $T_\pm^m$, (the absolute square of the polarization eigenmode eigenvalues) has to be modified as the follows :

$$T_\pm^m = \left| \left(iA_m \sin\Delta\delta_{NL} \pm \sqrt{(\sqrt{E^2+F^2}-E)/2} \right) + G_m \cos\Delta_{NL} \pm \sqrt{(\sqrt{E^2+F^2}+E)/2} \right|^2 \quad (8)$$

where $A_m = \cos(\delta/2)\cos(\delta_1/2)$ - $\cos 2B\sin(\delta/2)\cos 2A \times\cos 2B_1\cos 2A_1\sin(\delta_1/2)$ - $\sin 2B\sin(\delta/2)\sin 2B_1 \times\sin(\delta_1/2)$, $G_m = \sin 2A\cos 2B\sin(\delta/2)\sin 2A_1\cos 2B_1 \times\sin(\delta_1/2)$, $E=[1-(G_m)^2-(A_m)^2]\sin^2\Delta\delta_{NL}+(G_m)^2$ - $(\sin 2A\cos 2B\sin(\delta/2))^2$, and $F = -2A_m\sin\Delta\delta_{NL}G_m \times\cos\Delta\delta_{NL}$.

Eq.(8) has a much more complicated form than Eq. (4), and cannot give a simple understanding of the birefringence effects inside the linear loop. When the birefringence inside the linear loop is purely linear and aligned to the optical axis, Eq.(8) can be expressed as

$$\lambda_\pm = ia_1 \sin\Delta\phi_{NL} \pm \sqrt{(1-a_1^2)\sin^2\Delta\phi_{NL} - c^2} \quad (9)$$

where $a_1 = a\cos\delta_1/2 - b\sin\delta_1/2$.

In case that the pump power is low, $T_\pm \approx c^2 = \sin 2A\cos 2B\sin(\delta/2)$, and the transmittance becomes independent of the birefringence inside the linear loop. The numerical results of Eq. 9 in Fig. 18 show that the effect of the birefringence inside the linear loop on the laser characteristics are very weak.

We now discuss the polarization characteristics for

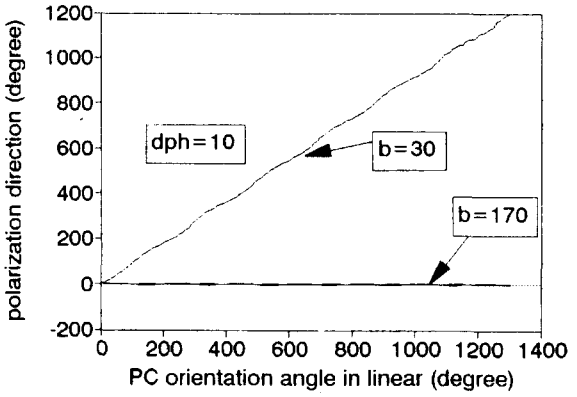

FIG. 18. The polarization directions of fiber lasers as a function of PC orientation angle inside the linear loop with various birefringence magnitudes(dotted line curve; 170°/m, solid line curve ; 30°/m).

polarization eigenmodes. When the linear loop has no birefringence, polarization eigenmodes are obtained as follows:

$$u_\pm = \frac{i(\sin 2B\sin\Delta_{NL} + \cos 2B\sin 2A\cos\Delta\phi_{NL})}{i\cos 2A\cos 2B\sin\Delta\phi_{NL} \pm \sqrt{(\cos^2 2B\cos^2 2A + \sin^2 2B)\sin^2\Delta\phi_{NL} - \cos^2 2B\sin^2 2A\cos^2\Delta\phi_{NL}}} \quad (10)$$

Eq.(10) shows that the polarizations of polarization eigenmodes are generally elliptical for small nonlinear phase shift. When $\Delta\delta_{NL} \approx 0.0$, $u_{\pm} \approx \begin{pmatrix} 1 \\ \pm 1 \end{pmatrix}$, and the polarization states of polarization eigenmodes are linear and does not depend on the birefringence inside the NALM. The phase difference between eigenmodes are dependent on the birefringence and PMB frequency cannot be observed in CW laser mode. When the linear loop has elliptical birefringence with parameters, δ_1, A_1, B_1, the components of eigenmodes have very complicated form. When nonlinear phase shifts are small,

$$u_{\pm} \approx \begin{bmatrix} \cos(\delta_1/2) + i\cos 2B_1 \sin 2A_1 \sin(\delta_1/2) \\ \sin 2B_1 \sin(\delta_1/2) \pm \sqrt{1 - \cos^2 2B_1 \sin^2 2A_1 \sin^2(\delta_1/2)} \end{bmatrix} \tag{11}$$

This equation shows that the states of polarization depend only on the birefringence of the linear loop. After some straightforward calculations from Eq. (11) with relations between parameters of the polarization state, the direction, θ_g, and the ellipticity of polarization eigenmodes, B_g, can be obtained as,

$$\theta_g = [\tan^{-1}(\cot(\delta_1/2)\csc(2B_1)]/2$$

and

$$B_g = \left[\sin^{-1}\left(\frac{\cos 2A_1 \cos 2B_1 \sin(\delta_1/2)}{\sqrt{1-(\sin 2A_1 \cos 2B_1 \sin(\delta_1/2))^2)}}\right)\right]/2.$$

When $B_1 = 0.0$ and $A_1 = 0.0$ for the purely linearly birefringent fiber inside the linear loop, $\theta_g = \pi/4$ and $B_g = \delta_1/4$. When the birefringence inside the linear loop is nearly circular, i.e., $B_1 \approx \pi/4$ and $A_1 = 0.0$, $\theta_g \approx \delta_1/4$ and $B_g \approx 0.0$. Fig. 18 shows the polarization direction, θ_g, as a function of PC orientation angle inside the linear loop, with various magnitudes of the birefringence inside linear loop. With weak birefringence (below about 30°/m), the polarization direction is found to rotate at about 0.5 of the rotation rate. The greater the magnitude of linear birefringence inside the fiber, the more tightly the polarization direction is located near the birefringence axis [15], when PC orientation changes. Fig. 19 and Fig. 20 show that these theoretical predictions (see solid line curves in Fig. 19 and Fig. 20) for the direction of polarization agree with the experimental results (see asterisk data curves in Fig. 19 and Fig. 20).

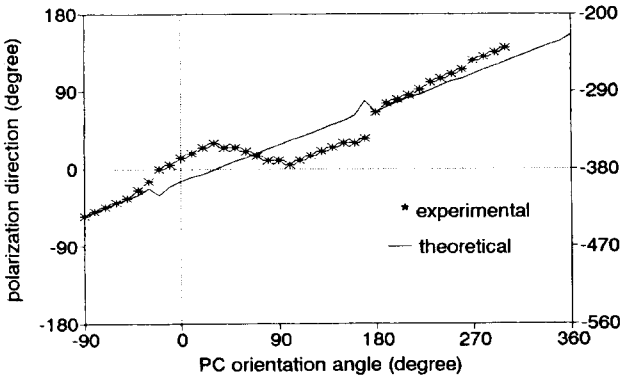

FIG. 20. The polarization directions of fiber lasers at 1555 nm as a function of PC orientation angle inside the linear loop (stars; experimental, solid line curve; theoretical, 50°/m).

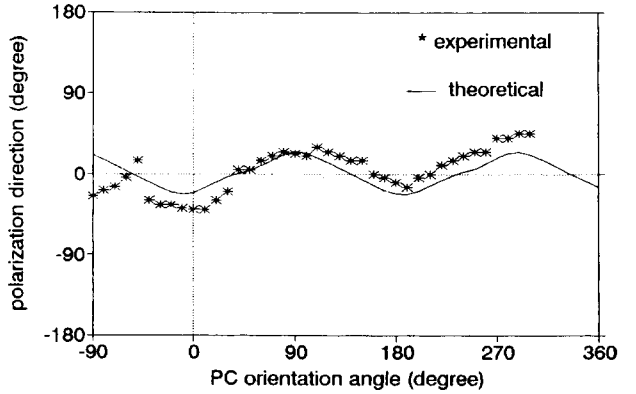

FIG. 19. The polarization directions of fiber lasers at 1545 nm as a function of PC orientation angle inside the linear loop (stars; experimental, solid line curve; theoretical, 28.9°/m).

III. CONCLUSIONS

In conclusion, we have theoretically analyzed and experimentally observed the effects of the wavelength dependent birefringence inside a figure eight cavity on fiber laser output characteristics. Using simplified models for the birefringence and laser dynamics, the output power and center wavelength of a figure eight cavity fiber laser were found to be a function of the magnitude of linear birefringence and nonlinear phase shift of the NALM. When the orientation of the polarization controller inside the NALM changes, optical power and center wavelength of the continuous wave oscillates periodically at low pump powers. The birefringence of a linear loop has little influence on the optical power and center wavelength of the laser output, but plays a major role in determining the polarization

properties of fiber lasers.

ACKNOWLEDGMENTS

The authors would like to acknowledge Dr. H. K. Lee of the research department in ETRI for technical assistance.

REFERENCES

[1] I. N. Duling III, Elecron. Lett. **27**, 544 (1991).
[2] A. G. Bulushev, E. M. Dianov, and O. G. Okhotnikov, Opt. Lett. **16**, 88 (1991).
[3] D. J. Richardson, R. I. Laming, D. N. Payne, V. J. Matsas, M. W. Phillips, Electrons Lett. **27**, 1451 (1991).
[4] I. N. Duling III, Opt. Lett. **16**, 539 (1991).
[5] K.H.Kim, M.Y. Jeon, S.Y. Park, H.K.Lee, and E. H. Lee, ETRI J. **18**, 1 (1996).
[6] H. Lin, D. K. Donald, and W. V. Sorin, J. Lightwave. Technol. **12**, 1121 (1994).
[7] A. J. Stentz, and R. W. Boyd, Opt. Lett. **19**, 1462 (1994).
[8] R. Ulrich, and A. Simon, Appl. Opt. **18**, 2241 (1979).
[9] N. Eickhoff, Y. Yen, and R. Ulrich, Appl. Opt. **20**, 3428 (1981)
[10] P. K. A. Wai and C. R. Menyuk, J. Lightwave. Technol. **14**, 148 (1996).
[11] H. Y. Kim, S. K. Kim, H. J. Jeong, H. K. Kim, and B. Y. Kim, Opt. Lett. **20**, 386 (1995).
[12] H. Haus, E. P. Ippen, and K. Tamura, IEEE J. Quantum Electron. **30**, 200 (1994).
[13] G. Stephan, R. Le Naour , and A. Le Floch, Phys. Rev. **A17**, 733 (1977).
[14] N. Mancier, A. Chankari, P. Meyrueis, and M. Clement, Appl. Opt. **34**, 6489 (1995).
[15] H. Y. Kim, El Hang Lee, and B. Y. Kim, Appl. Opt. **36**, 6764 (1997).